

# **EXAFS by itself and in good company**

**Victor Krayzman**  
(NIST)

**EXAFS-50 Symposium**

A. I. Kostarev, Zh. Eksp. Teor. Fiz. 11, 60 (1941).  
A. I. Kostarev, Zh. Eksp. Teor. Fiz. 20, 811 (1950);  
V. V. Shmidt, Zh. Eksp. Teor. Fiz. 39, 1269 (1960) [Sov. Phys. JETP 12, 886 (1961) ]  
I. B. Borovskii and G. N. Ronami, Bull. Acad. Sci. USSR, Phys. Ser. 21, 1385 (1957)  
I. B. Borovskii and G. N. Ronami Bull. Acad. Sci. USSR, Phys. Ser. 25, 1008 (1961)  
I. B. Borovskii, V. A. Batyrev, and A. I. Kozlenkov, Bull. Acad. Sci. USSR, Phys. Ser. 27, 387 (1963)  
I. B. Borovskii, Bull. Acad. Sci. USSR, Phys. Ser. 27, 830 (1963)  
B. A. Batyrev, Bull. Acad. Sci. USSR, Phys. Ser. 27, 389 (1963)  
G. N. Ronami and O. N. Shirkin, Bull. Acad. Sci. USSR, Phys. Ser. 27, 824 (1963)  
I. B. Borovskii and V. V. Shmidt, Bull. Acad. Sci. USSR, Phys. Ser. 25, 994 (1961)  
V. V. Shmidt, Bull. Acad. Sci. USSR, Phys. Ser. 25, 988 (1961)  
A. I. Kozlenkov, Bull. Acad. Sci. USSR, Phys. Ser. 25, 968 (1961)  
A. I. Kozlenkov, Bull. Acad. Sci. USSR, Phys. Ser. 27, 373 (1963)

## EXAFS spectroscopy: a new method for structural investigation

I. B. Borovskii, R. V. Vedrinskiĭ, V. L. Kraĭzman, and V. P. Sachenko

*Institute of Solid-State Physics of the Academy of Sciences of the USSR, Chernogolovka, Moscow region*

*M. A. Suslov State University, Rostov*

Usp. Fiz. Nauk **149**, 275–324 (June 1986)

EXAFS spectroscopy is a new method of investigating materials which allows one to determine structural parameters of the local environment of atoms with some specified  $Z$  by studying their x-ray spectra. Among these parameters are the interatomic spacings, coordination numbers and amplitudes of thermal oscillations. It is not necessary for long-range order to be present in the sample under investigation. Depending on the way this technique for obtaining the spectrum is applied, one can analyze the local environment of atoms located either within the sample volume or at its surface. We investigate the physical phenomena on which the method is based, the mathematical techniques used to process the experimental data, and various methods of recording the spectra. We present a series of examples in which EXAFS spectroscopy is used to study superionic conductors, compounds with intermediate valence, biological molecules, solid solutions, catalysts, surface layers and intercalated compounds.

### TABLE OF CONTENTS

Introduction.....	539
1. Methods for experimental investigation .....	540
2. Theoretical description of EXAFS .....	543
2.1. Single-scattering and single-particle approximations. 2.2. The influence of many-electron effects on the EXAFS lineshape. 2.3. Theoretical determination of atomic phases and scattering amplitudes. 2.4. The influence of thermal and structural disorder on EXAFS. 2.5. Principles of processing EXAFS data and the effect of multiple scattering.	
3. Methods of processing EXAFS data.....	552
3.1. Obtaining the normalized EXAFS from an experimental spectrum. 3.2. Problems in the choice of $E_0$ and determination of the function $\chi(k)$ . 3.3. Fourier analysis of the function $\chi(k)$ and determination of contributions from different coordination spheres. 3.4. Extracting the contribution of a given coordination sphere for a Gaussian radial atomic-pair distribution function. 3.5. Obtaining the radial atomic-pair distribution function.	
4. Experimental investigations and applications of EXAFS-spectroscopy.....	557
4.1. Comparison of theory with experiment. 4.2. Application of EXAFS to the investigation of atomic structure.	
Conclusion .....	566
References.....	567

## Laboratory diffractometer-based XAFS spectrometer

A.T.Shuvaev, B.Yu.Helmer, T.A.Lyubeznova,  
V.A.Shuvaeva

*Institute of Physics, Rostov State University, Stachki  
194, Rostov-on-Don, 344090, Russia.*

*E-mail: vshuvaev@uic.rnd.runnet.ru*

The device has been developed to allow XAFS spectra of good quality to be obtained using conventional powder diffractometer. The device is based on the mechanical system which synchronizes the changes of curvature radius of bent crystal-monochromator with the Bragg angle. Due to high resolution (1-10 eV depending on the wavelength) and photon flux only several hours are needed to perform quality XAFS experiment. The device is easy to operate and can be successfully used both for XAFS investigations and for student's practice.

**Keywords:** XAFS spectrometer, XAFS laboratory experimental facilities

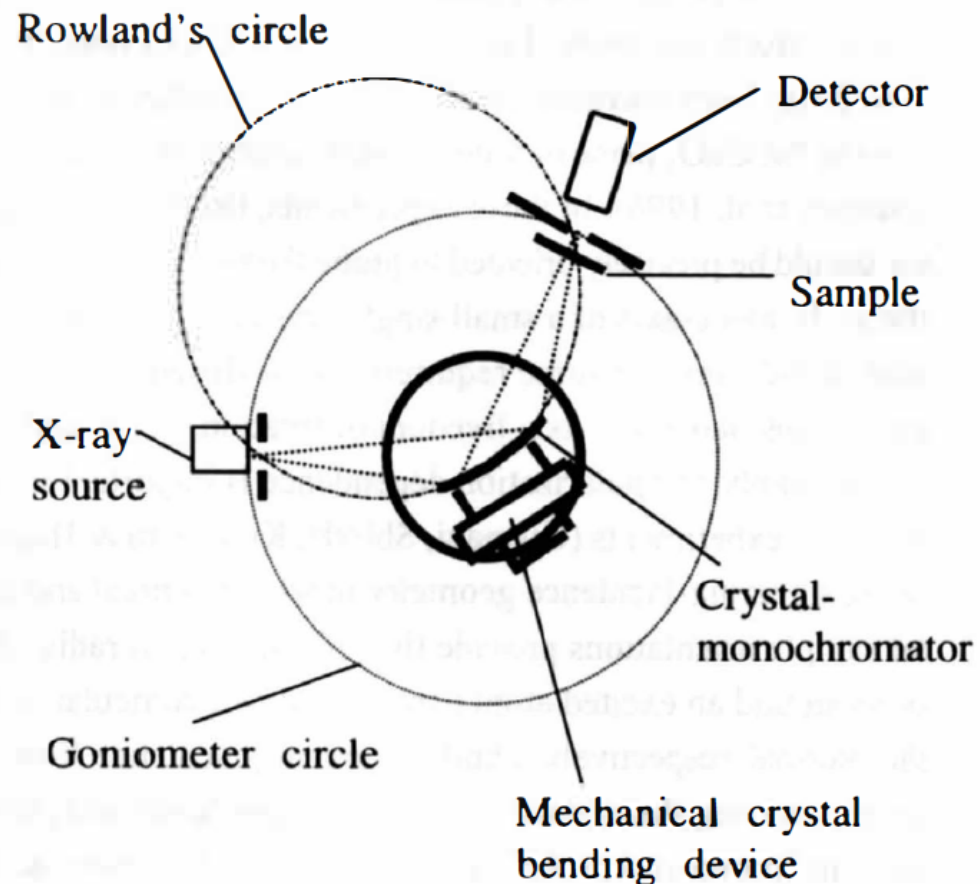


**Figure 1**  
Schematic view of the laboratory diffractometer-based XAFS spectrometer

## **EXAFS study of graphite intercalation compound with transition metals (Fe,Ni)**

Shuvaev A.T. , Khelmer B.Y., Lyubeznova T.A., Kraizman V.L., Mirmilstein A.S., Kvacheva L.D., Novikov Yu. N. and Volpin M. E.

J. Phys. France **50**, 1145 (1989)

## **Study of dynamics of iron trichloride hydration and oxidation by the x-ray absorption-spectroscopy technique.**

Shuvaev A.T. , Khelmer B.Y., Lyubeznova T.A., Kraizman V.L., Novakovich A.A.

KHIMICHESKAYA FIZIKA, (Chemical physics Sov.) **10**, 516-523 (1991)

Babanov Yu.A., Vasin V.V., Ageev V.V., Ershov N.V.  
Phys. Stat. Sol. B **105**, 747 (1981)

$$\chi_K^{(\alpha)}(k) = -4\pi\rho \sum_{\beta} c_{\beta} \frac{|f_{\beta}(k, \pi)| Z_K^{(\alpha)}}{k} \int_0^{\infty} g_{\alpha\beta}(R) e^{-\frac{2R}{\lambda}} \sin(2kR + 2\delta_1^{(\alpha)} + \vartheta_{\beta}) dR$$

$$N_{\alpha\beta}(R_1, R_2) = 4\pi\rho c_{\beta} \int_{R_1}^{R_2} r^2 g_{\alpha\beta}(r) dr$$

$$I(s) = 1 + \frac{4\pi\rho}{sF_0^2(s)} \sum_{\alpha} \sum_{\beta} c_{\alpha} F_{\alpha}(s) c_{\beta} F_{\beta}(s) \int_0^{\infty} (g_{\alpha\beta}(r) - 1) \sin(sr) r dr$$

$$s = 4\pi \sin(\theta) / \lambda$$

# Reverse Monte Carlo

## RMCPprofile software package

Data sets for powder samples

1. Neutron total scattering in R space and in Q space
2. X-ray total scattering in R space and in Q space
3. Bragg profile
4. EXAFS

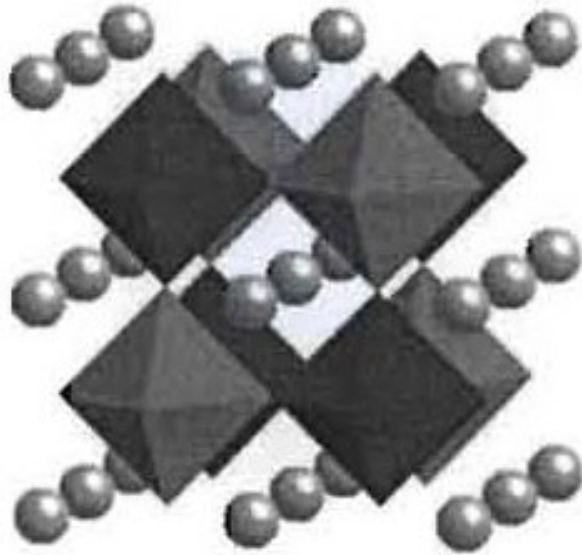
Electron, X-ray, and neutron diffuse scattering for single crystals

Metropolis algorithm for minimization of total residual  $R = \sum w_i R_i$

# A combined fit of total scattering and extended X-ray absorption fine structure data for local-structure determination in crystalline materials

V. Krayzman,<sup>a,b</sup> I. Levin,<sup>a\*</sup> J. C. Woicik,<sup>a</sup> Th. Proffen,<sup>c</sup> T. A. Vanderah<sup>a</sup> and M. G. Tucker<sup>d</sup>

<sup>a</sup>Ceramics Division, National Institute of Standards and Technology, Gaithersburg, MD 20899, USA, <sup>b</sup>Department of Materials Science and Engineering, University of Maryland, College Park, MD 20742, USA, <sup>c</sup>Lujan Neutron Center, Los Alamos National Laboratory, Los Alamos, NM, USA, and <sup>d</sup>ISIS, Rutherford Appleton Laboratory, Didcot, UK. Correspondence e-mail: igor.levin@nist.gov



SrAl<sub>1/2</sub>Nb<sub>1/2</sub>O<sub>3</sub> structure



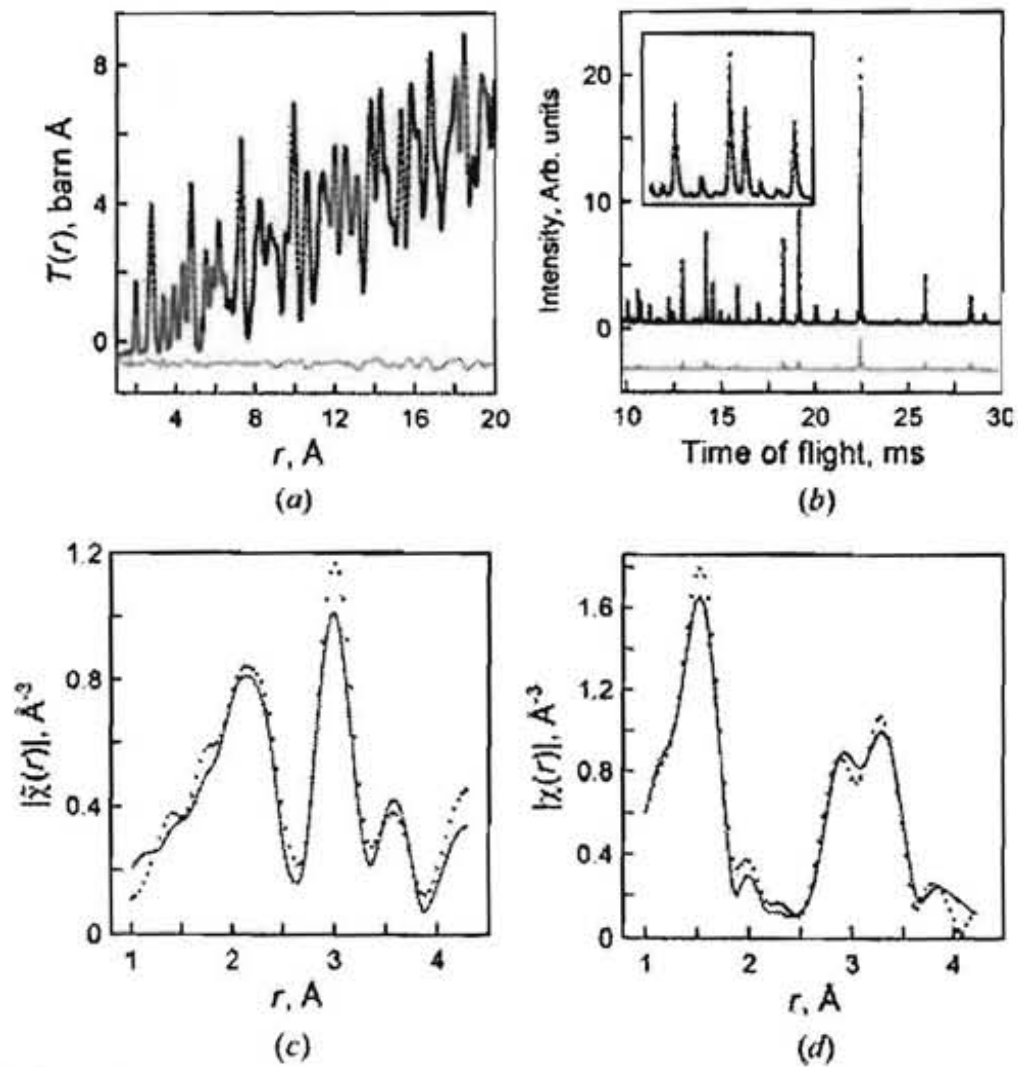


**Figure 4**

Experimental (dotted lines) and calculated (solid lines) (a)  $T(r)$ , (b) Bragg, and (c) Sr EXAFS and (d) Nb EXAFS profiles for  $\text{SrAl}_{1/2}\text{Nb}_{1/2}\text{O}_3$  obtained by a simultaneous RMC fit. The inset in (b) displays a magnified view of the high- $Q$  range of the Bragg profile. The  $k$  ranges used in EXAFS Fourier transforms were  $3.3\text{--}13.2 \text{ \AA}^{-1}$  for Nb and  $3.0\text{--}14.2 \text{ \AA}^{-1}$  for Sr.

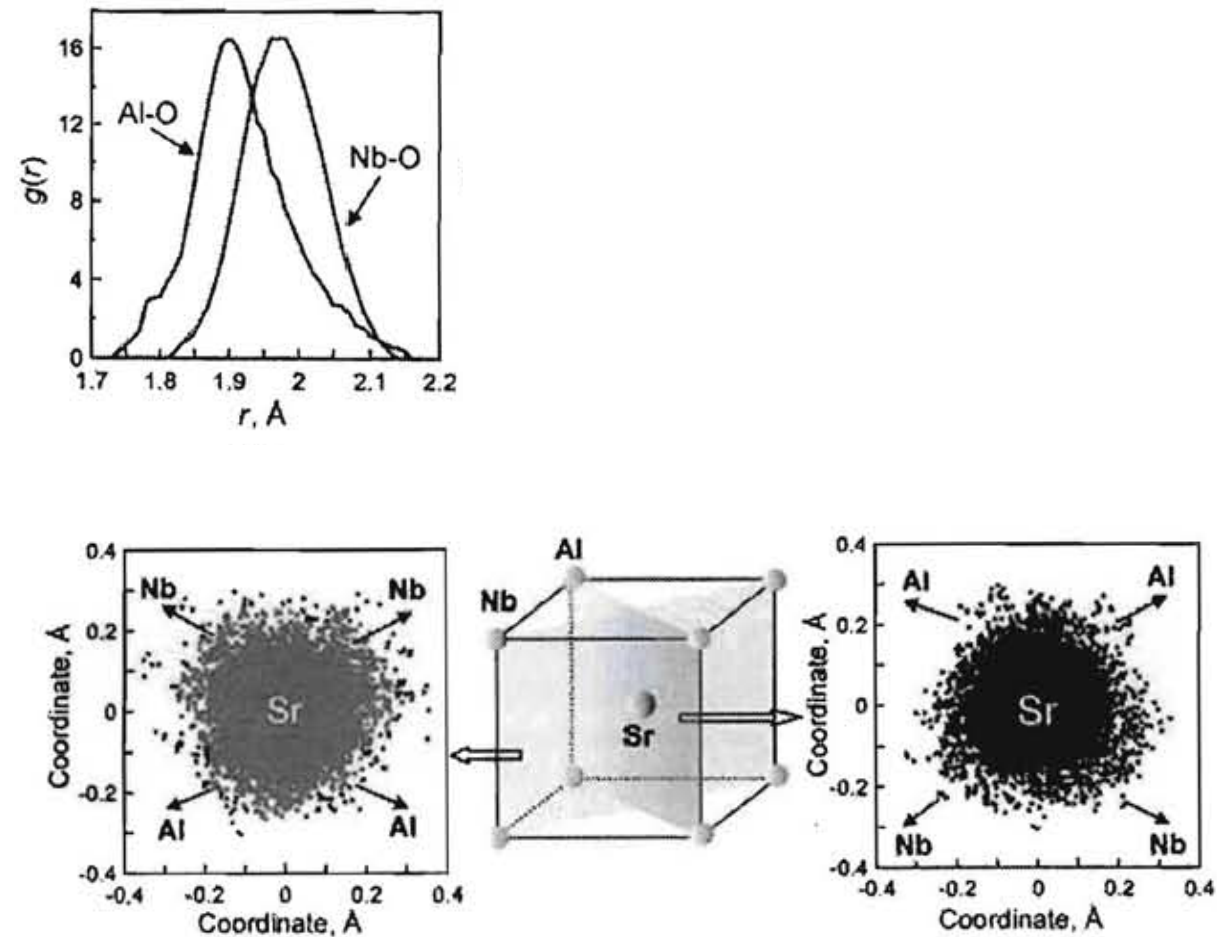


**Figure 10**

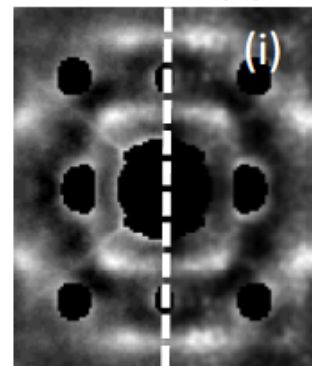
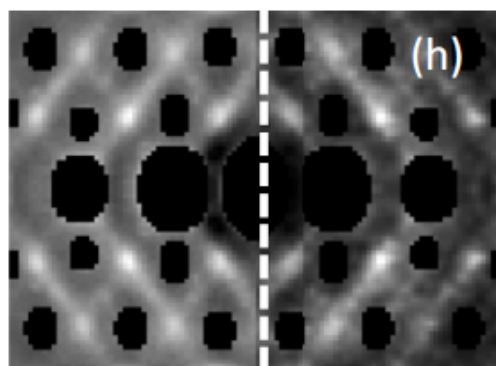
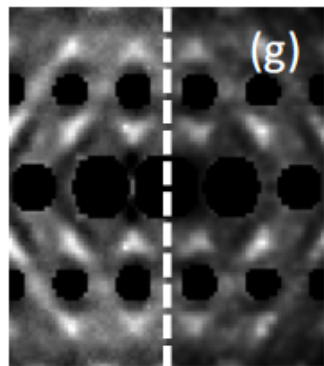
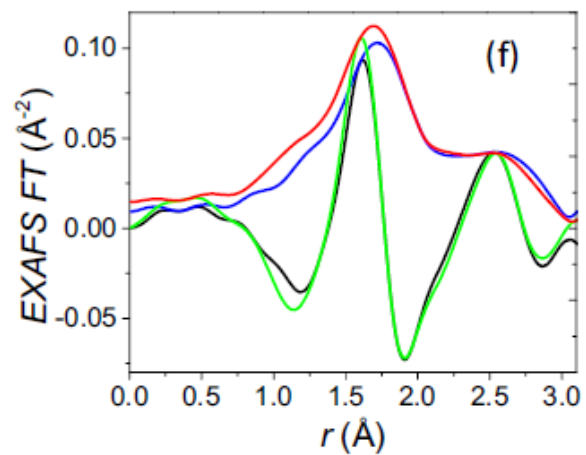
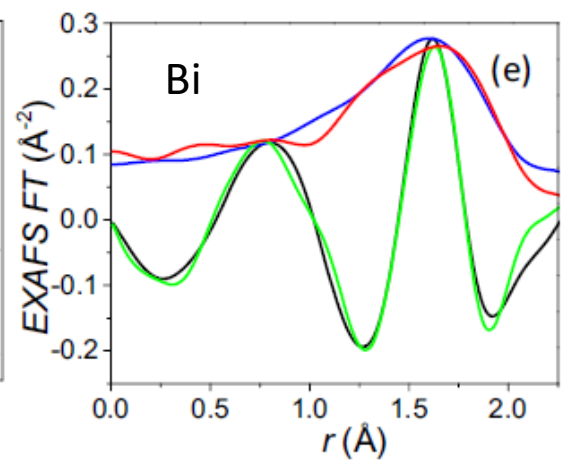
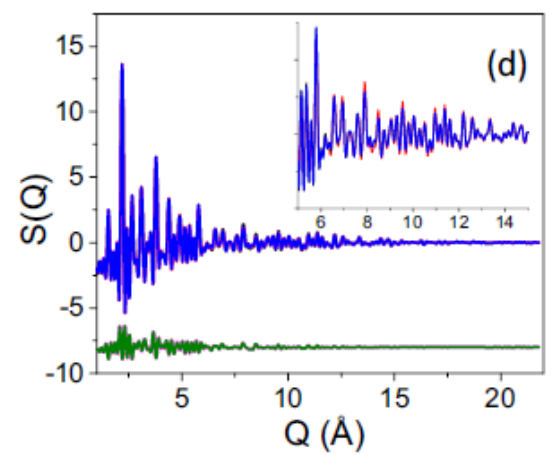
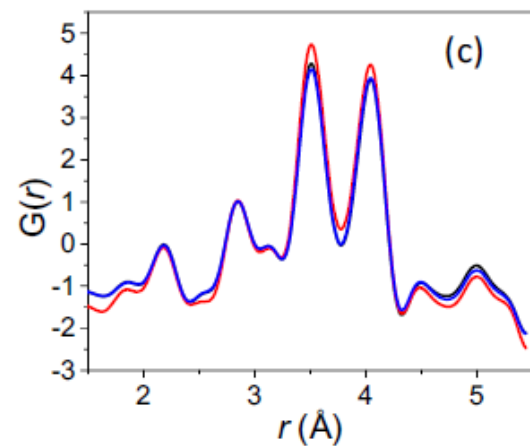
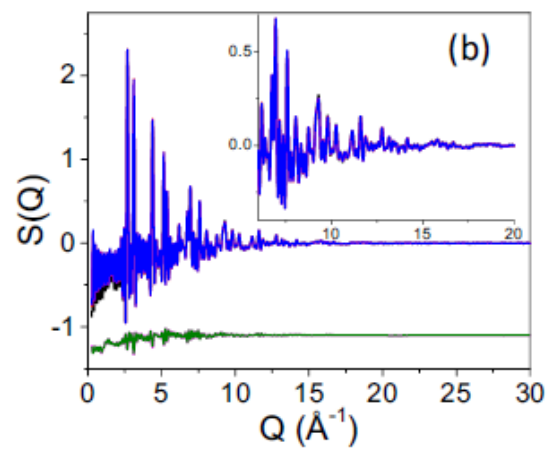
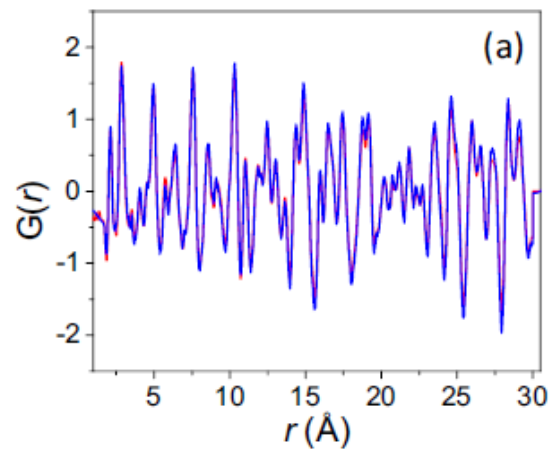
(Middle) Schematic drawing of the Sr coordination by Nb and Al in SAN. (Left, right) Projections of the Sr probability density function on the  $[110]$  and  $[\bar{1}\bar{1}0]$  sections, respectively. Each point in these plots represents an instantaneous Sr position. Arrows indicate the directions toward the neighboring B cations. A pronounced complementary asymmetry of the two sections is observed.

PHYSICAL REVIEW B **93**, 104106 (2016)

## **Local structure in BaTiO<sub>3</sub>-BiScO<sub>3</sub> dipole glasses**

I. Levin, V. Krayzman, J. C. Woicik, F. Bridges,  
G. E. Sterbinsky, T-M. Usher, J. L. Jones, and D. Torrejon

(Ba<sub>0.6</sub>Bi<sub>0.4</sub>)(Ti<sub>0.6</sub>Sc<sub>0.4</sub>)O<sub>3</sub> solid solutions



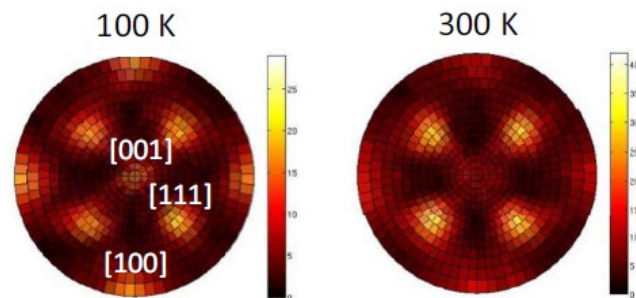
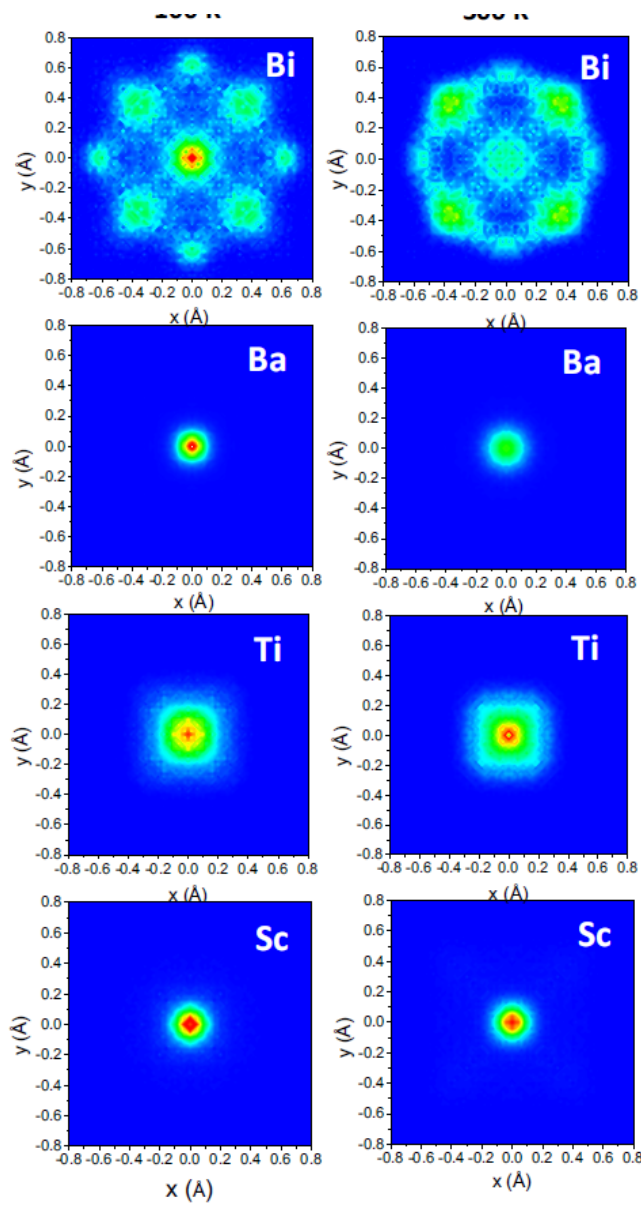


FIG. 16. Stereographic projections displaying the PDDs for directions of the Bi displacements at 100 K and 300 K. These distributions exhibit well-defined maxima for the  $\langle 111 \rangle$  and  $\langle 100 \rangle$  directions. The relative probability of  $\langle 111 \rangle$  displacements is larger at 300 K.

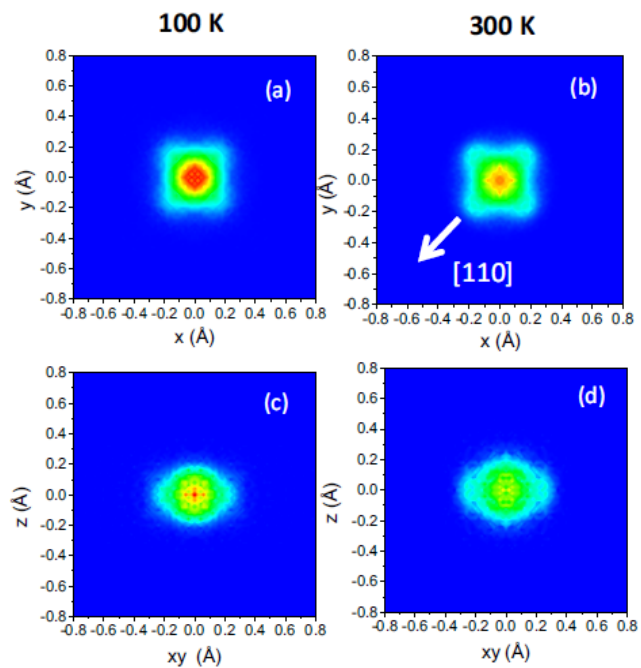


FIG. 17. (a–b) PDDs of oxygen atoms projected onto  $\{001\}$  plane; (c–d) a  $\{110\}$  slice through this PDD.

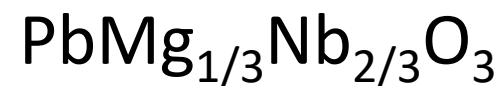
ARTICLE

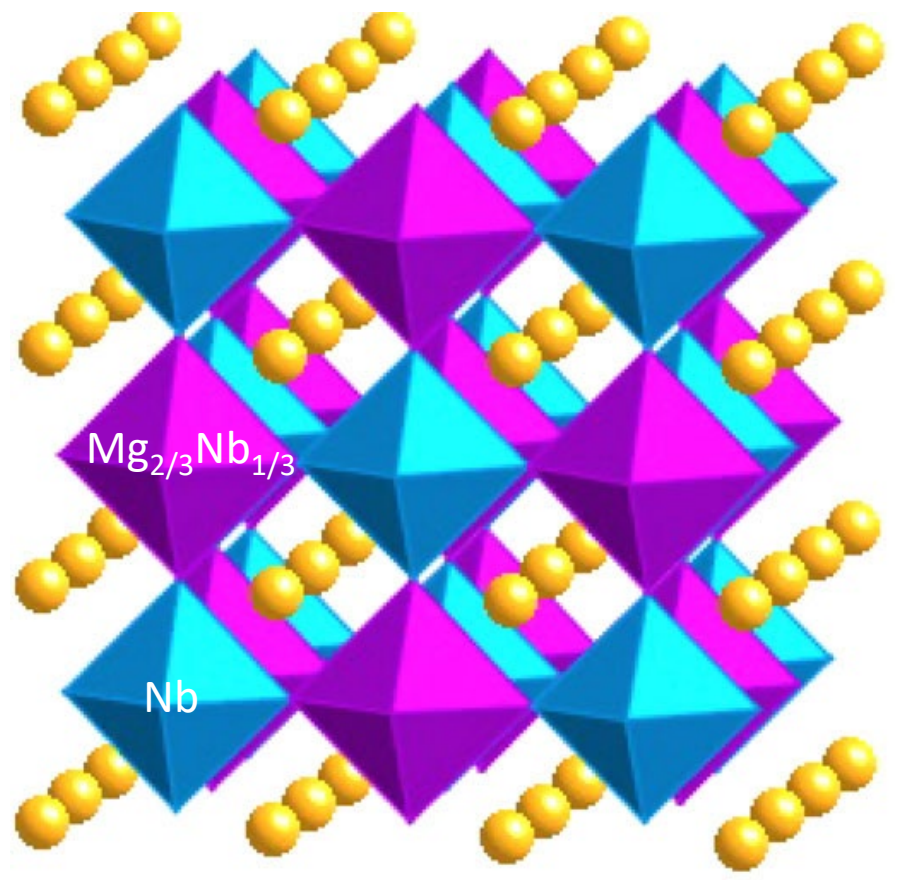
<https://doi.org/10.1038/s41467-019-10665-4>

OPEN

# Local atomic order and hierarchical polar nanoregions in a classical relaxor ferroelectric

M. Eremenko<sup>1</sup>, V. Krayzman<sup>1</sup>, A. Bosak<sup>2</sup>, H.Y. Playford<sup>3</sup>, K.W. Chapman<sup>4</sup>, J.C. Woicik<sup>1</sup>, B. Ravel<sup>1</sup> & I. Levin<sup>1</sup>

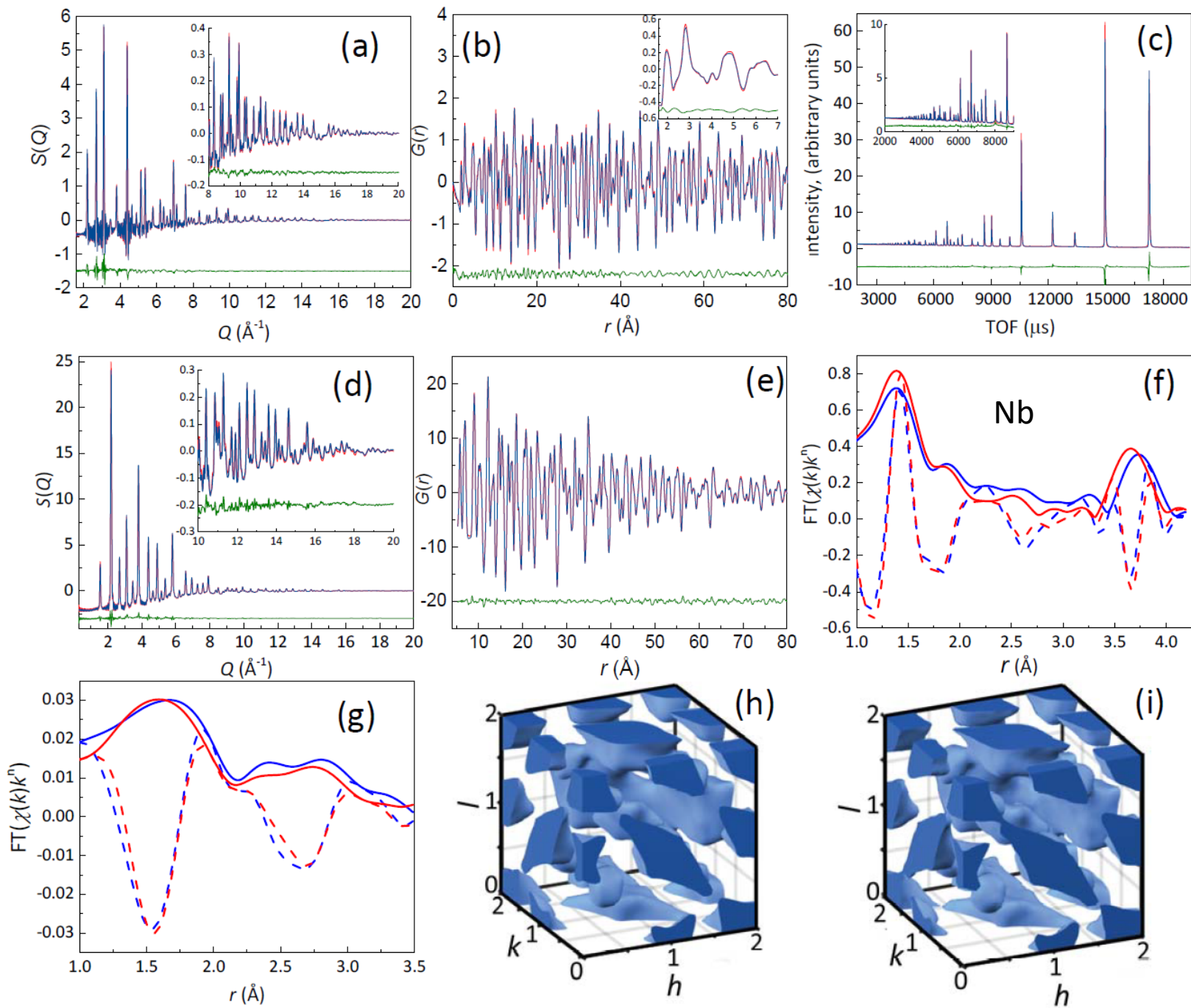


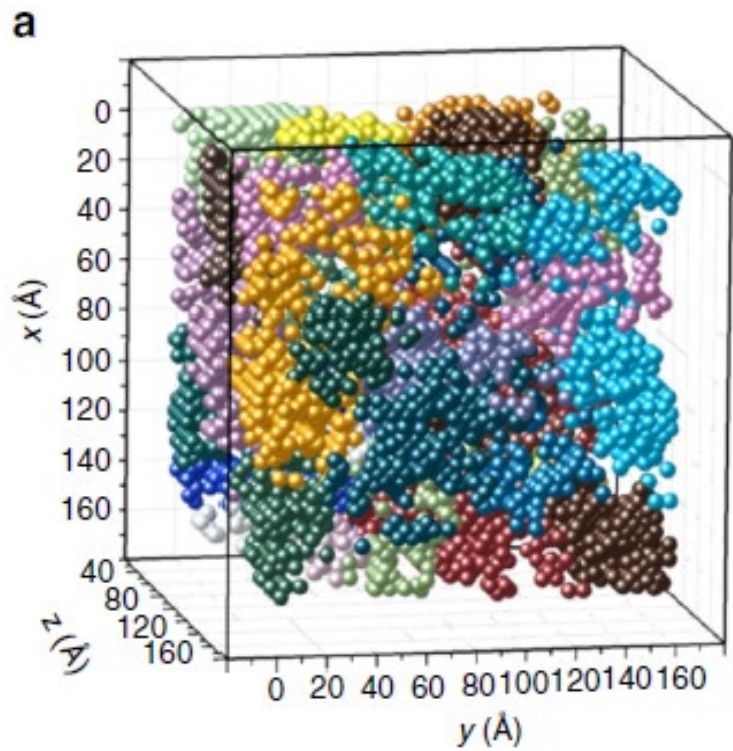


Mg<sub>2/3</sub>Nb<sub>1/3</sub>

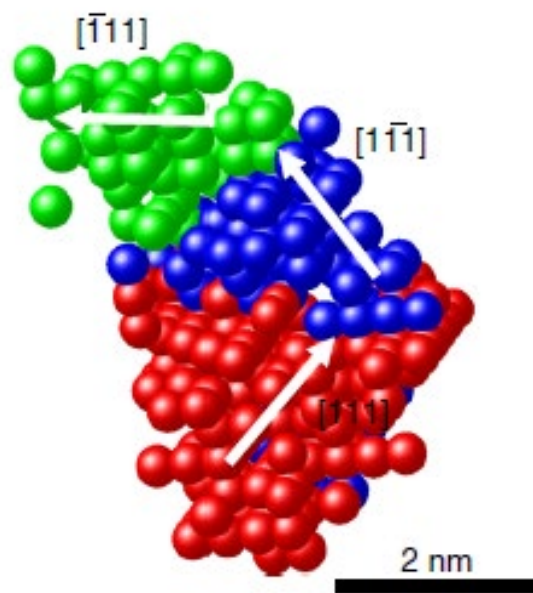
Nb

313600 atoms  
160 Å x 160 Å x 160 Å





$\alpha$  PNR



$\langle 111 \rangle$  PNR



R. Vedrinskii  
A. Mirmilstein  
A. Novakovich  
L. Bugaev  
A. Shuvaev  
B. Khelmer (Chudnovsky)  
A. Vazina

I. Levin  
M. Eremenko  
Y. Zhang  
M. Tucker

Thank you for attention